Kobe University Repository : Kernel

PDF issue: 2026-11-05

Separation of particle-laden oil-in-water emulsion using swirling flows formed by an in-line separator

Kurimoto, Ryo
Kimura, Tohru
Hayashi, Kosuke
Takimoto, Hideya

(Citation)
Chemical Engineering Research and Design,225:321-327

(Issue Date)
2026-01

(Resource Type)
journal article

(Version)
Version of Record

(Rights)
© 2025 The Author(s). Published by Elsevier Ltd on behalf of Institution of Chemical Engineers.
This is an open access article under the Creative Commons Attribution-NonCommercial-NoDerivatives 4.0 International license

(URL)
https://hdl.handle.net/20.500.14094/0100498959

Chemical Engineering Research and Design 225 (2026) 321–327

Contents lists available at ScienceDirect

Chemical Engineering Research and Design

journal homepage: www.elsevier.com/locate/cherd

Separation of particle-laden oil-in-water emulsion using swirling flows formed by an in-line separator

Ryo Kurimoto [a], Tohru Kimura [a], Kosuke Hayashi [a,*], Hideya Takimoto [b]

[a] Graduate School of Engineering, Kobe University, 1-1, Rokkodai, Nada, Kobe, Hyogo, Japan
[b] MORIGO SEIKI CO., LTD., 10-2, Minamifutami, Futami, Akashi, Hyogo, Japan

ARTICLE INFO

Keywords:
Swirling flow
Separation
O/w emulsion
Particles
Vertical pipe

ABSTRACT

This paper presents the capability of an in-line separator, which forms a swirling flow in a vertical pipe, to enhance separation of three-phase mixture, i.e., particle-laden oil-in-water emulsion, into each phase. First, the separation of the oil-in-water emulsion without fine particles was confirmed to be enhanced due to the swirling flow. The swirl angle and the radial distribution of particles in a swirling flow were measured by image processing for efficient separation of fine particles from the liquid phase; these measurements were useful to understand effective separation of the solid-liquid mixture using a pick-off ring (POR), which extracts the mixture flowing along the pipe wall. Finally, experiments on the separation of three-phase mixture demonstrated a prospect for effective phase separation of the three-phase mixture in a swirling pipe flow.

1. Introduction

Industrial washing machines remove oil and chips from the surfaces of machined products by either immersion in cleaning liquids (with or without ultrasonic cleaning) or spraying with cleaning liquids. The amount of oil droplets and chips in a cleaning liquid increases during iterative usage. The cleaning liquid usually contains surfactant for enhancing oil removal. The presence of surfactant suppresses coalescence between oil droplets, so that the liquid becomes an oil-in-water emulsion. Users of the washing machines expects to extend their life in the view of reducing disposal costs and environmental burden. Thus, it is required to develop efficient separating methods for oil droplets and chips from cleaning liquids.

Swirling flows have been widely used in separation of each phase from mixture, e.g., gas-liquid phases (Kataoka et al., 2008; Matsubayashi et al., 2012; Qiu et al., 2024), oil-water phases (Hamza et al., 2020; Bu et al., 2024), liquid-solid phases (Yang et al., 2010; Syed et al., 2017). There are several devices to form a swirling flow. Cyclonic separators are one of representative devices for centrifugal separation. They must be set beside an existing piping system so that an additional space is required for their installation. Compared to other devices, in-line separators consisting of separation parts and a swirler, which has a hub and stationary vanes with an inclination, have the advantage that they can be installed easily in existing piping systems. In addition, no additional power source is required to form a swirling flow using them if the flow rate of the system is sufficient for separation without significant increase in the pressure drop. There are some reports that oil droplets even with the diameter of about 100 μm in water were separated using in-line separators (Hamza, et al., 2020; Liu et al., 2024). Chips in a cleaning liquid would be easier to separate than oil droplets due to their size and density. The in-line separators, therefore, have a potential to simultaneously separate a mixture of chips, oil droplets, and cleaning liquid. However, the separation of a three-phase mixture, i.e., particle-laden oil-in-water emulsion, has not been sufficiently investigated. In the present study, three kinds of separation experiments were carried out to examine the capability of an in-line separator: (1) verification of enhanced separation of oil-in-water emulsion, (2) verification of fine particle separation in water with visualization of particle distribution in a swirling flow to examine the enhancement of separation performance, and (3) verification of simultaneous separation of oil and fine particles in particle-laden oil-in-water emulsion building upon the findings of (1) and (2). This study supports United Nations Sustainable Development Goals (SDG), particularly SDG 6, SDG 9, and SDG 12 by advancing cleaner, more efficient, and chemical-free separation methods that enhance water quality, promote sustainable industrial practices, reduce waste, and help prevent pollution (Fegade, L.,2024a).

* Corresponding author.
E-mail address: hayashi@mech.kobe-u.ac.jp (K. Hayashi).

https://doi.org/10.1016/j.cherd.2025.12.012
Received 2 October 2025; Received in revised form 3 December 2025; Accepted 6 December 2025
Available online 8 December 2025
0263-8762/© 2025 The Author(s). Published by Elsevier Ltd on behalf of Institution of Chemical Engineers. This is an open access article under the CC BY-NC-ND license (http://creativecommons.org/licenses/by-nc-nd/4.0/).

2. Experimental method

2.1. Oil-water separation

Fig. 1(a) shows the experimental setup for oil-water separation experiments. It consists of the vertical pipe, the in-line separator consisting of the swirler and the oil separation tube, the oil separation tank, the emulsion return pipe, the upper tank, the lower tank, and the liquid supply system. The vertical pipe was made of transparent acrylic resin. Its diameter D and length were 20 and 600 mm, respectively. Emulsion was supplied by the pump (IWAKI, MD-70R) and its flow rate was measured by the flowmeter (NIPPON FLOW CELL, NFLT-R-CB00). The swirler formed a swirling flow of the emulsion in the vertical pipe. The swirler was removed when data of non-swirling flows were obtained as reference. The oil separation tube shown in Fig. 1(b) located at the center of the pipe and its bottom end was $z = 300$ mm, where z is the axial coordinate in the pipe and $z = 0$ at the top of the swirler. The inner and outer diameters of the tube were 6 and 8 mm, respectively. Tap water, non-soluble cutting oil (ENEOS, DM20), and surfactant (MORIGO SEIKI, MC-20) were mixed to make emulsion using the pump and the return pipe to the lower tank for 10 min (Yasuda and Haneda, 2015). The emulsion was left to stand for 2 h and was mixed again for 10 min just before starting an experiment. We presumed that oil droplets move toward the center of the pipe due to the swirling flow since the density of oil (845 kg/m^3) was lighter than that of water. Thus, we expected that an oil rich emulsion could be collected using the oil separation pipe. The emulsion was circulated through the setup for four hours during an experiment. Experiments were carried out at room temperature and atmospheric pressure. The temperature of liquids was kept at 298 ± 1 K.

Fig. 1(c) shows the schematic of the oil separation tank storing collected emulsion. Oil droplets in the emulsion rose by the buoyant force due to the difference in the density. Consequently, a separated oil layer was formed upon the emulsion layer. The emulsion return pipe, consisting of vertical inner and outer pipes, was used to return only the emulsion in the emulsion layer to the lower tank. The emulsion entered the annular gap between the outer and inner pipes through bottom holes and was subsequently discharged through the top of the inner pipe, flowing downward along its inner surface. The separation of oil from the emulsion was evaluated by measuring the thickness δ_o of the separated oil layer in the oil separation tank. The δ_o was measured based on camera images of the tank from the horizontal direction at each hour until four hours. Fig. 2 shows an example of measured δ_o. The measured δ_o linearly increased with time t. The time series of δ_o were expressed by a linear regression line and its gradient was defined as the separation rate R_o:

$$\delta_o = R_o t + c \tag{1}$$

where c is the constant for linear regression.

Fig. 3 shows the swirler shape, which was designed based on a swirler for gas-liquid separation (Koto et al., 2022; Koto et al., 2023). It was made of photopolymer resin using a stereolithography 3D-printer (FLASH FORGE, FFT-060) and had 12 stationary vanes with the vane angle of 80° at the flow outlet.

The composition of the emulsion is listed in Table 1. The ratio of oil in Case 2 is slightly larger than that in Case 1. The flow rate Q_E of the emulsions ranged from 1.1×10^{-4} to 4.3×10^{-4} m^3/s, which was determined based on the nominal flow rate of a cleaning liquid in an actual industrial washing machine. The average velocity u_k of a mixture was defined by

$$u_k = \frac{Q_k}{A} \tag{2}$$

where A is the cross-sectional area of the pipe and the subscript k denotes each mixture ($k = E$, S, or SE; E: emulsion; S: solid-water mixture; SE: solid-emulsion mixture). The Rynolds number Re_k was defined by

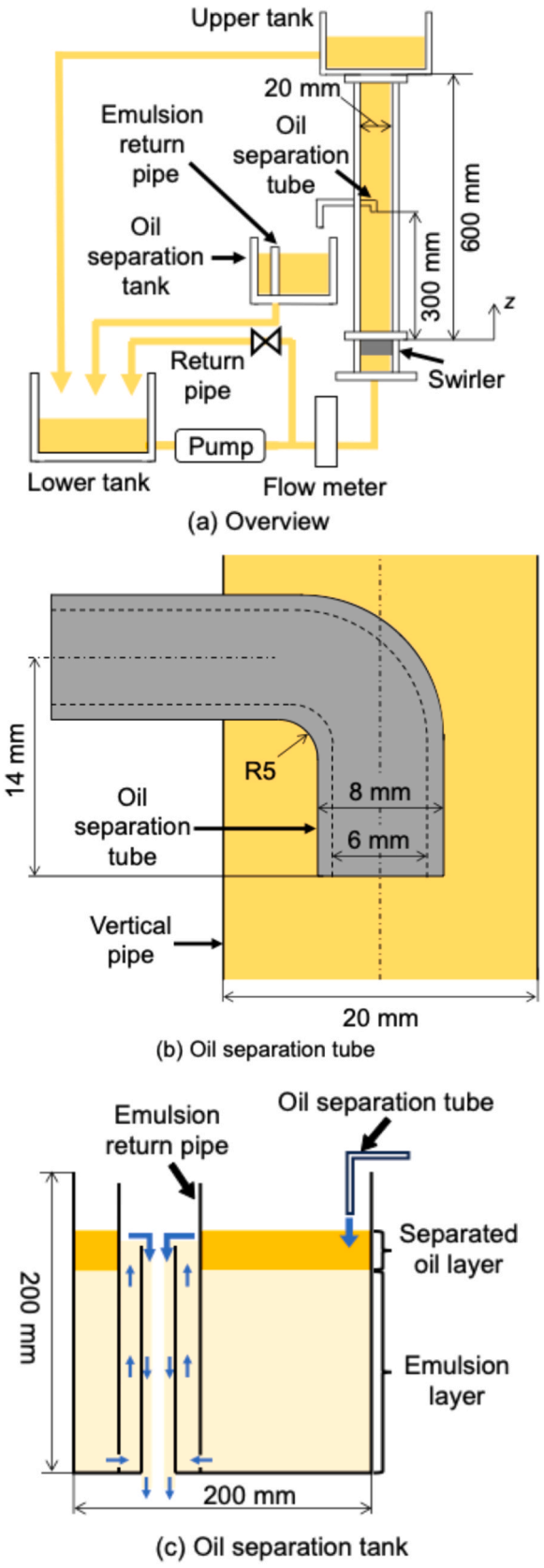


Fig. 1. Experimental setup for oil-water separation.

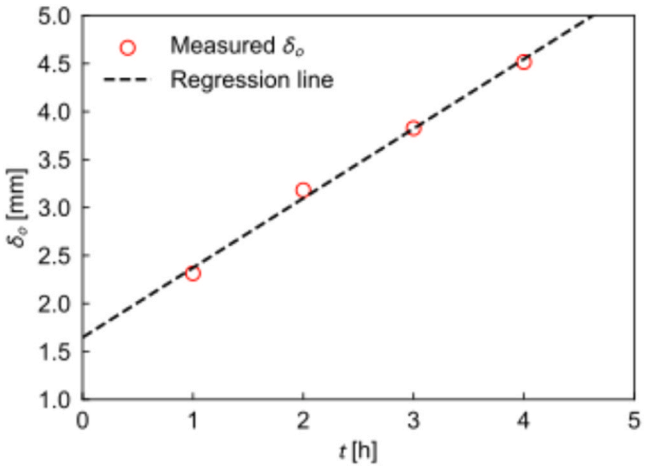


Fig. 2. Relation between measured δ_o and t.

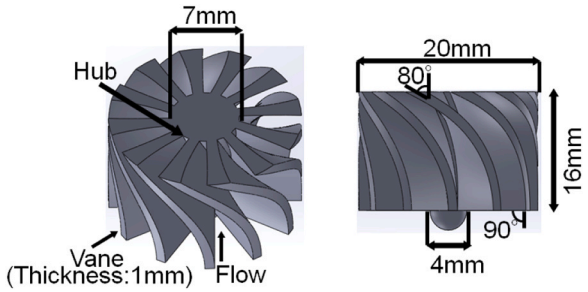


Fig. 3. Swirler shape.

Table 1
Composition of o/w emulsion (vol%).

	Oil	Surfactant	Water
Case 1	8	5	87
Case 2	12	5	83

$$\mathrm{Re}_k = \frac{\rho_k u_k D}{\mu_k} \tag{3}$$

where ρ and μ are the density and viscosity of mixture, respectively. The ρ_E and μ_E were measured using the electronic balance (SHIMADZU, UW4200H) and the viscometer (A&D, SV-10), respectively. The Re_E ranged from 5800 to 23000 in Case 1 and from 8500 to 33000 in Case 2. Therefore, emulsion flows in the pipe were in a turbulent state.

2.2. Solid-water separation

2.2.1. Separation experiment

Fig. 4(a) shows the experimental setup for solid-water separation experiments. The vertical pipe, the swirler, the upper tank, and the lower tank were the same as those for the oil-water separation experiment. The pick-off ring (POR) and the solid separation tank were installed. The POR, which was designed based on one for gas-liquid separation (Koto et al., 2022; Koto et al., 2024), could separate the solid-water mixture flowing near the pipe wall and the separated mixture was stored in the solid separation tank without return. The unseparated mixture reached to the reservoir tank after passing through the upper tank. Thus, this experiment was once-through in a condition.

The schematic of the POR is illustrated in Fig. 4(b). The gap δ between the outer wall of the POR and the inner wall of the pipe was 0.5 or 1.0 mm. The POR located at $z = 80$ or 180 mm to discuss the effect of swirl angle on the separation rate.

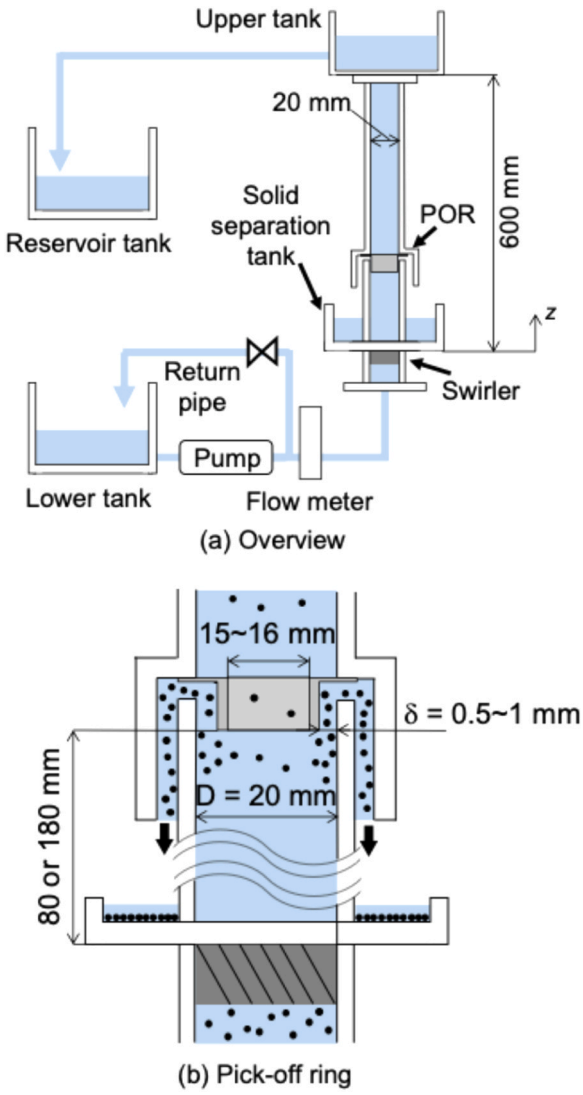


Fig. 4. Experimental setup for solid-water separation.

Glass beads were used for the solid phase. Their mean diameter was 100 μm and their density was 2570 kg/m^3. The mass fraction of the glass beads was 3 wt% and they were well mixed using the pump and the return pipe. We measured the mass fraction of the glass beads in the solid separation tank after experiments to evaluate the separation performance. The flow rate Q_S of solid-water mixture was 1.2×10^{-4} m^3/s. The flows of solid-water mixture were in a turbulent state since the Reynolds number Re_S of the solid-water mixture was 8000, where ρ_S was measured using the densimeter and μ_S was evaluated by the correlation proposed by Tsuchiya et al. (1997).

2.2.2. Swirl angle and particle distribution measurements

The radial distribution of particles and the swirl angle in the pipe were measured using a high-speed camera (PHOTRON, FASTCAM Mini AX50) and illumination sources as shown in Fig. 5. The laser with a cylindrical lens was used to generate a laser sheet parallel to the camera angle for the measurement of the radial distribution of particles. The laser sheet passed the axis of the pipe. The frame rate and the number of images were 2000 frames/s and 20000, respectively. Brightness at each pixel in the range of $z = z_0 \pm 2.5$ mm, where z_0 is the measurement elevation, was averaged at each radial coordinate r and then the time averaged brightness $b(r)$ was calculated. When the camera recorded particles for the measurement of the swirl angle, the LED light was used

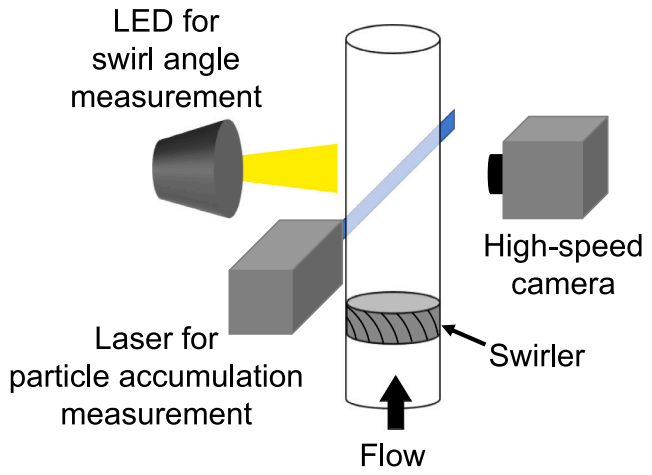


Fig. 5. Layout for image recording of particles.

as a backlight without the laser sheet. The focus of the camera lens was adjusted at the front side of the pipe to record particles flowing at the front side. The frame rate and the number of images taken were 2000 frames/s and 2000, respectively. The particle image velocimetry (PIV) (Koto et al., 2023) was applied to recorded images to calculate the radial and axial components, v_r and v_z, of a velocity. The swirl angle θ was defined by $\theta = \tan^{-1}(v_r/v_z)$. The processed region was on the axis line of the pipe and the interrogation area was 60 × 60 pixels.

2.3. Three-phase separation

Fig. 6 shows the experimental setup for three-phase separation experiments. The setup is a combination of the experimental setups for the oil-water and solid-water separation. The solid separation tank had the emulsion return pipe, which returns emulsion near the free surface, so that unseparated three-phase mixture circulated in the setup during the experiment. The bottom end of the oil separation tube located at $z = 300$ mm. The location of the POR was determined based on results in the solid-water separation experiment as will be discussed in Section 3. Glass beads of 3 wt% were included in the emulsion of Case 1. They were mixed using the pump and the return pipe for 10 min, and then left to stand for 2 h. After that, the emulsion-solid mixture was mixed again for 10 min just before starting each experiment. During the experiment, the mixture in the lower tank was stirred with a mixer for 10 min every 30 min. The separation rate of oil was evaluated by the separated oil layer thickness in the oil separation tank and that of solid was evaluated by the mass of particles in the solid separation tank. The flow rate Q_{SE} of three phase mixture was 1.1×10^{-4} m^3/s. The Reynolds number Re_{SE} of three phase mixture was 5800, i.e., turbulent flow, where ρ_{SE} was measured using the densimeter and μ_{SE} was evaluated by the Tsuchiya correlation with μ_E.

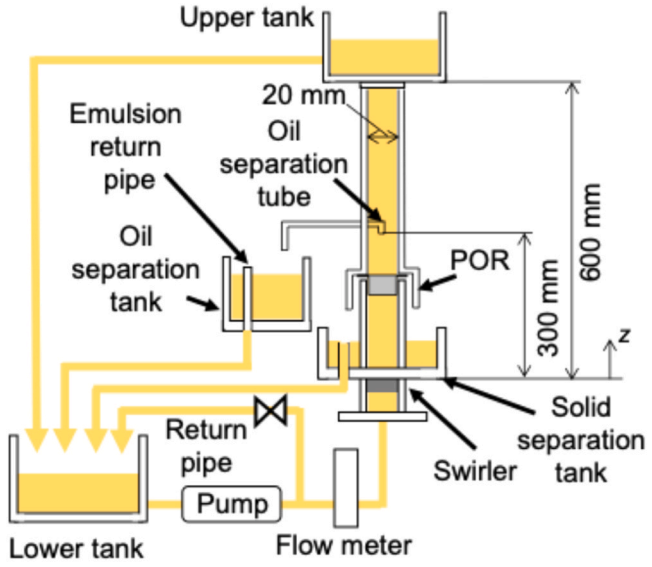


Fig. 6. Experimental setup for three-phase separation.

3. Results and discussion

3.1. Oil-water mixture

3.1.1. Gravity separation of oil from water in ampoule

In advance of swirling flow experiments, the effect of gravity on separation was confirmed by measuring the thickness of a separated oil layer upon the emulsion in an ampoule. The time series of the separation ratio in the ampoule, which is the ratio of the thickness at each time to that at the end of the observation (96 h), are shown in Fig. 7. The separation gradually proceeded in both cases and the curves of the separation ratio became a plateau exceeding 80 h. This indicates that the separation of the emulsion only by gravity takes extremely long time in both cases. Compared with these data, the separation ratio in Case 1 of Table 1 is lower than that in Case 2 until 50 h, indicating that the lower oil fraction leads to the formation of a more stable emulsion. The larger oil fraction is likely to increase the number of droplets and decrease the surfactant concentration on droplet interfaces. The former and latter contribute to ease contact between droplets and ease rupture of their liquid film, respectively. Therefore, coalesced droplets are likely to rise, and the separation is enhanced.

3.1.2. Oil-water separation

Fig. 8 shows R_o of the oil-water emulsion in swirling and non-swirling flows. The error bars in the figure represent the standard deviation. The R_o in swirling flows are higher than those in non-swirling flow for all Q_E. The R_o in swirling flows slightly increases with increasing Q_E, whereas Q_E dependence of R_o in non-swirling flows is not remarkable. The droplet collection using the oil separation tube depends on the centrifugal force acting on droplets. The magnitude of the centrifugal force F_C acting on a fluid particle of the phase i is expressed by

$$F_{Ci} \sim \rho_i d^3 \frac{v_t^2}{r} \tag{4}$$

where d is the dimeter of the fluid particle, and v_t the tangential velocity of the fluid particle. The centrifugal force acting on oil droplets with lighter density is lower than that on water with heavier density. Oil

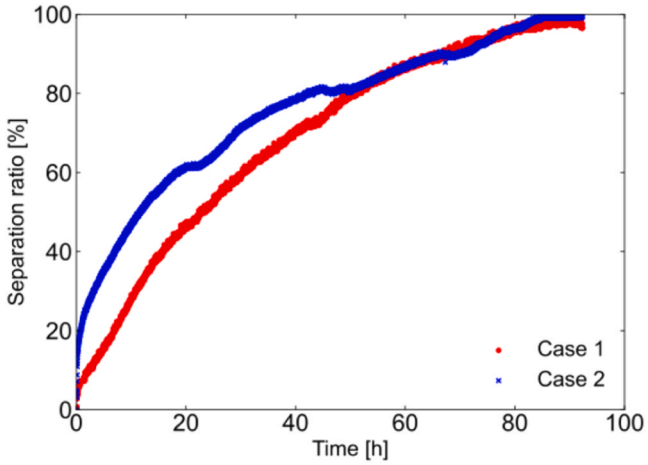


Fig. 7. Separation of oil from emulsion by gravity in ampoule.

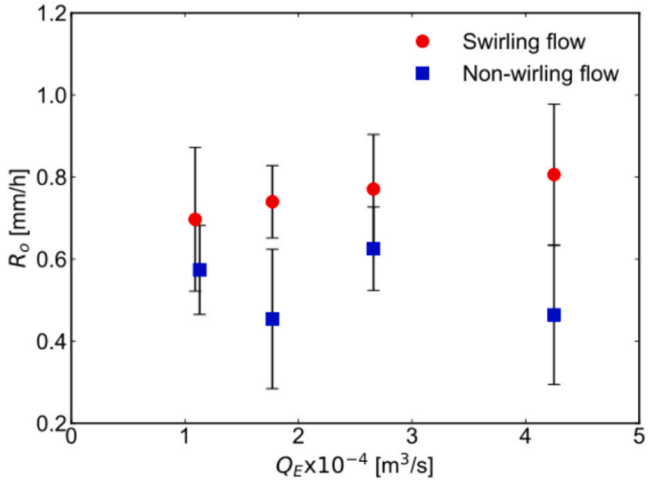


Fig. 8. Effects of swirling flow on R_o in Case 1.

droplets thus migrate toward the center of the pipe due to the smaller centrifugal force compared with water. The present types of swirlers would contribute to the increase in v_t with increasing Q_E (Koto et al., 2022; Koto et al., 2024). Therefore, the oil separation is enhanced due to the increase in Q_E.

Fig. 9 exhibits the comparison of R_o between Cases 1 and 2 in swirling flows. The R_o in Case 2 is larger than that in Case 1 at all Q_E. Oil droplets in Cases 1 and 2 were observed using a microscope and their images are shown in Fig. 10. The number of large droplets is clearly larger in Case 2 than in Case 1. The F_C is proportional to d^3, whereas the drag force, which is the counter force of F_C, is proportional to d^2. Thus, the increase in d from Case 1 to Case 2 enhances the migration of droplets toward the center of the pipe. In addition, the large droplets are ease to form a thicker separated oil layer in the oil separation tank due to large buoyant force as shown in Fig. 7, which also contributes to the higher R_o.

These experiments demonstrated that the present in-line separator enhances the separation of the oil-water emulsion.

3.2. Solid-water mixture

3.2.1. Swirl angle and radial distribution of particles

The variation of θ with respect to z^* ($= z/D$) is shown in Fig. 11. The θ linearly decreases as z^* increases. This indicates that swirl motion decays with increasing z^* due to the wall friction, and this result is

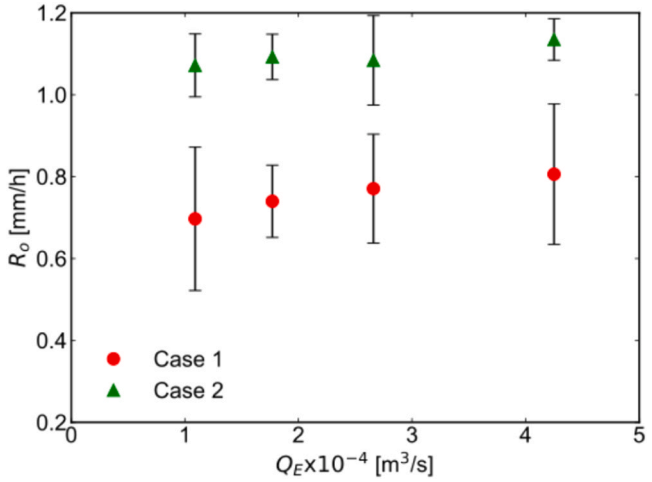


Fig. 9. Comparison of R_o between Cases 1 & 2 in swirling flows.

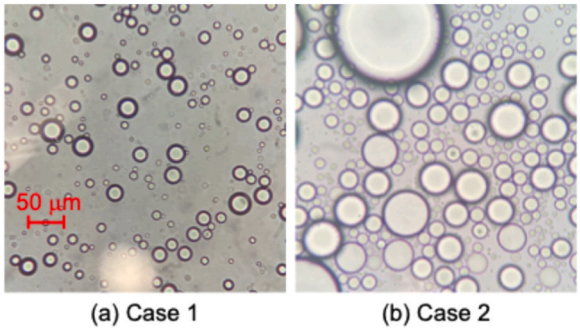


Fig. 10. Oil droplets observed by microscope.

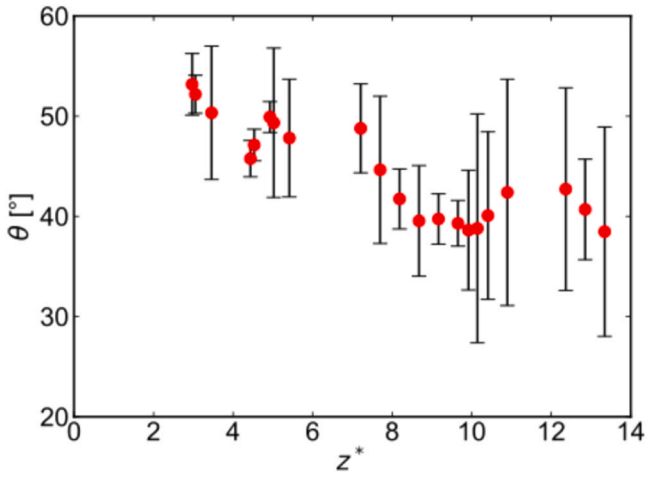


Fig. 11. Swirl angle.

consistent with findings reported in the literature (Hatazawa, 1998; Kitoh, 1991; Yajnik and Subbaiah, 1973).

Fig. 12 shows the radial distribution of b^* ($= b(r)/b_a$) in swirling and non-swirling flows at $z^* = 4$, where b_a is the average of b in the radial direction, and r^* ($= r/R$) the dimensionless radial coordinate. Here, R is the pipe radius. The b^* is uniform in the non-swirling flow. In contrast, b^* in the swirling flow drastically increases for $r^* > 0.8$, clearly showing that the swirl motion causing the centrifugal force makes the particles migrate to the near-wall region.

The particle accumulation rate K within the gap δ of POR to be used in the particle separation test is evaluated by

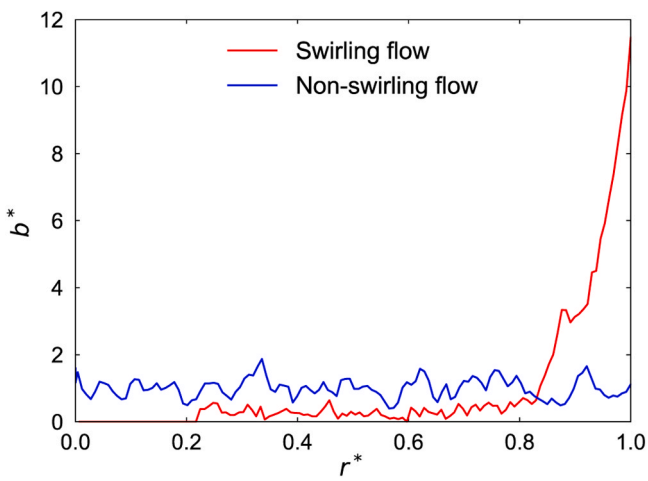


Fig. 12. Radial distribution of particles at $z^* = 4$.

$$K = \frac{\int_{R-\delta}^{R} 2\pi brdr}{\int_{0}^{R} 2\pi brdr} \quad (5)$$

The variation of K at $\delta = 10$ mm with respect to z^* is shown in Fig. 13. The K in swirling flow is much larger than that in non-swirling flow and gradually tends to decrease as z^* increases. The decrease in K is caused by the decay of swirl motion with increasing z^* as shown in Fig. 11. In addition to its reduction tendency with respect to z^*, K periodically varies about 30 % between the short range of z^*, e.g., K drops from 60 % to 40 % and then rises up to 70 % for $2 < z^* < 4$. A shadowgraph image of the particle-laden flow is shown in Fig. 14. We observed two spiral bands of particle-dense (shaded by blue color for visibility) and particle-sparse regions alternatively with respect to z^*. The formation of the bands might relate to the presence of vanes in the swirler. Thus, the periodic variation of K is attributed to the bands. The circumferential locations of highly accumulated particle regions, i.e., particle dense bands, rotate in the circumferential direction with respect to z^* due to the swirling flows. Thus, circumferential averaged K would decrease without periodic variation as z^* increases. At $z^* = 4$, K takes the maximum value, which is attributed to particle migration from the center region for $z^* < 4$ and particle dispersion for $z^* > 4$ due to the decay of swirl intensity. Therefore, it is expected that the separation rate of particles depends on the location of the POR.

3.2.2. Solid-water separation

The mass fraction of separated particles in the solid separation tank is shown in Fig. 15. As shown in Fig. 4(b), the location of POR was changed at $z = 80$ or 180 mm corresponding to $z^* = 4$ and 9, respectively, and δ was 0.5 or 1.0 mm. The mass fraction in non-swirling flow does not depend on z^* and δ, since particles uniformly disperse in the radial direction regardless of z^*, as shown in Figs. 12 and 13. In contrast, the mass fraction in the swirling flows decreases with increasing δ and z^*. As shown in Fig. 12, the accumulation of particles weakens with increasing distance from the pipe wall. The wider δ permits a part of the flow with low particle concentration to pass the gap. Therefore, the mass fraction is lower at $\delta = 1.0$ mm than $\delta = 0.5$ mm in the swirling flows. As expected, the reduction in the mass fraction due to the increase in z^* is attributed to the decay of swirl motion. Thus, the distributions of the swirl angle and the particle accumulation are useful to achieve efficient design for collection of fine particles.

3.3. Three-phase separation

Based on the results in Section 3.2, the POR of $\delta = 0.5$ mm was set at $z^* = 4$ and then three-phase separation experiments were carried out. Fig. 16 shows the mass fraction of solid and emulsion in the solid separation tank. The mass fraction of solid is larger in the swirling flow than in the non-swirling flow, demonstrating that the separation of solid particles can be enhanced even in the three-phase flow using the in-line separator.

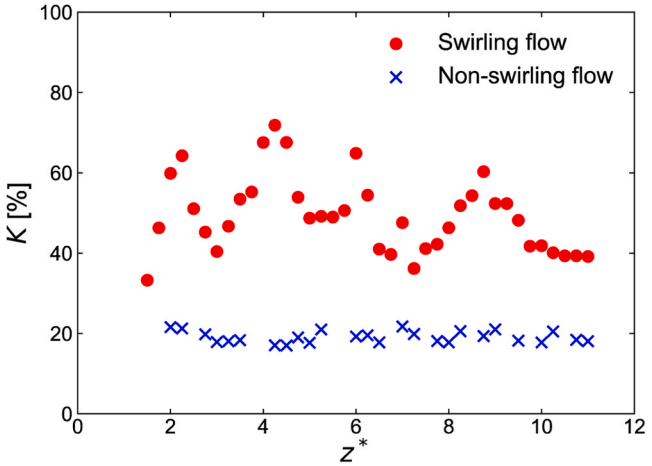


Fig. 13. Particle accumulation.

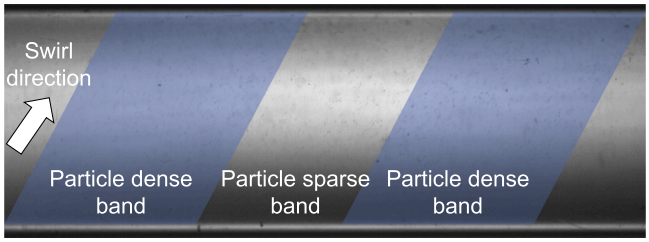


Fig. 14. Shadowgraph image of particle-laden swirling flow.

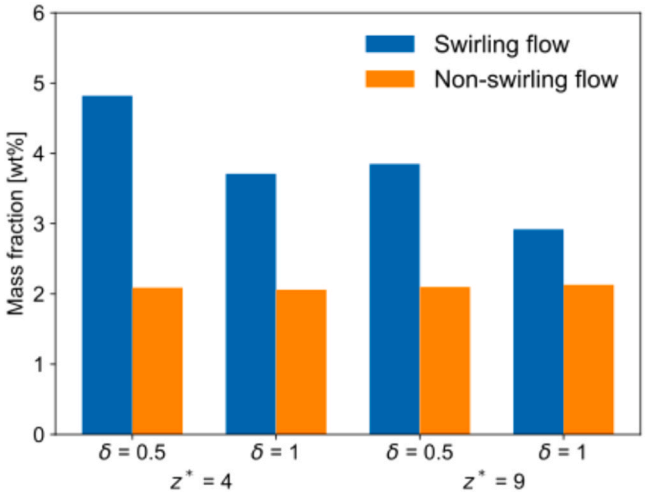


Fig. 15. Mass fraction of solid phase in separated mixture.

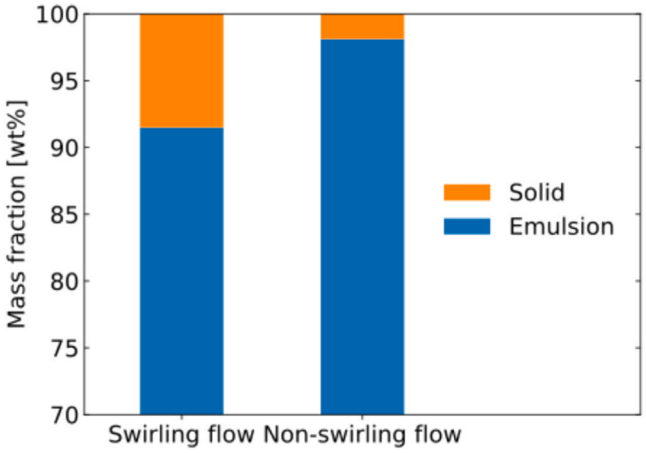


Fig. 16. Mass fraction of solid and emulsion in solid separation tank.

The R_o in the oil separation tank is shown in Fig. 17. The swirling flow enhances R_o even in the three-phase mixture. Therefore, the present in-line separator consisting of the swirler, the oil separation tube, and the POR has the prospect for the effective phase separation of particle-laden oil-in-water emulsion. The methodology of this study represents a green approach because it relies on physical separation techniques without hazardous chemicals, thereby aligning with key principles of green chemistry, specifically Principle 1 (Prevention), Principle 3 (Less Hazardous Chemical Syntheses), Principle 5 (Safer Solvents and

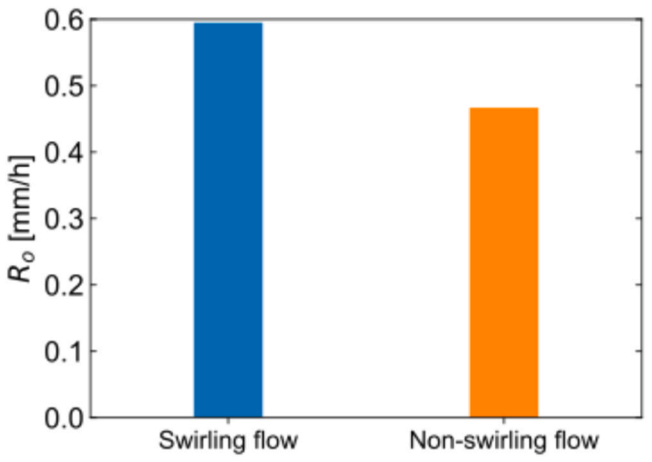


Fig. 17. Separation rate of oil phase from three phase mixture.

Auxiliaries), and Principle 6 (Design for Energy Efficiency) among the Twelve Principles of Green Chemistry (Fegade, 2024b).

4. Conclusion

The applicability of an in-line separator, consisting of a swirler, an oil separation tube, and a pick-off ring (POR) for the separation of three-phase mixture, i.e., particle-laden oil-in-water emulsion, was investigated experimentally. Before the separation of three-phase mixture, separation experiments on oil-in-water emulsion and solid-water mixture were carried out individually to investigate the possibility of the separation of each phase. In addition, the distributions of particles and the swirl angle were measured to understand the characteristics of swirl motion. The following conclusions were obtained:

(1) The swirling flow formed by the in-line separator enhanced the separation of oil from the oil-in-water emulsion. Its separation rate slightly increased with increasing the flow rate.
(2) The separation rate of solid particles from solid-water mixture depended on the location and gap width of the POR. Their separation performance could be understood based on the swirl angle and the radial distribution of particles.
(3) The in-line separator had the prospect for the enhancement of phase separation from the particle-laden oil-in-water emulsion.

The present study has dealt with a water-insoluble oil as the oil phase of the oil-in-water emulsion. Water-soluble oils are also widely used for cutting oil in machine tools. For enhancement of the applicability of the in-line separator, it would be worth investigating the separation performance for a three-phase mixture, i.e., water-soluble oils, cleaning liquid, and chips, in future works.

CRediT authorship contribution statement

Kosuke Hayashi: Writing – original draft, Supervision, Project administration, Methodology, Investigation, Funding acquisition, Formal analysis, Conceptualization. **Hideya Takimoto:** Writing – original draft, Methodology, Investigation, Funding acquisition, Conceptualization. **Tohru Kimura:** Writing – original draft, Visualization, Methodology, Investigation, Formal analysis, Data curation. **Ryo Kurimoto:** Writing – original draft, Visualization, Validation, Methodology, Investigation, Formal analysis, Conceptualization.

Declaration of Competing Interest

The authors declare that they have no known competing financial interests or personal relationships that could have appeared to influence the work reported in this paper.

Acknowledgement

The authors would like to express their gratitude to Mr. Kenta Akagi for his assistance in experiments. This work was supported by Research and Development Supporting Program for Growing Industry in Hyogo prefecture.

References

Bu, T., Mesa, D., Brito-Parada, P.R., 2024. Design strategies for miniaturised liquid–liquid separators - A critical review. Chem. Eng. J. 495, 153036.
Fegade, S., L, 2024a. Assessment of greenness of catalytic deoxygenation of crop oil for green diesel production. Clean. Circ. Bioeconomy 8, 100091.
Fegade, S.L., 2024b. Red chemistry: principles and applications, Next. Sustainability 4, 100048.
Hamza, J.E., Al-Kayiem, H.H., Lemma, T.A., 2020. Experimental investigation of the separation performance of oil/water mixture by compact conical axial hydrocyclon. Therm. Sci. Eng. Prog. 17, 100358.
Hatazawa, M., 1998. Characteristics of turbulent swirling flow in a straight pipe -Swirl effect on pressure loss-. J. Jpn. Soc. Fluid Mech. 17, 202–213.
Kataoka, H., Tomiyama, A., Hosokawa, S., Sou, A., Chaki, M., 2008. Two-phase swirling flow in a gas-liquid separator. J. Power Energy Syst. 2 (4), 1120–1131.
Koto, R., Kurimoto, R., Imaizumi, A., Hayashi, K., Tomiyama, A., 2022. Effects of swirl intensity on interfacial and wall friction factors of annular flows in a vertical pipe. Nucl. Eng. Des. 399, 112001.
Kitoh, O., 1991. Experimental study of turbulent swirling flow in a straight pipe. J. Fluid Mech. 225, 445–479.
Koto, R., Kurimoto, R., Hayashi, K., Tomiyama, A., 2023. Effects of liquid viscosity on interfacial and wall friction factors of swirling annular flows in a vertical pipe. Nucl. Eng. Des. 412, 112476..
Koto, R., Kurimoto, R., Hayashi, K., Tomiyama, A., 2024. Effects of pipe diameter on interfacial and wall friction factors of swirling annular flows in a vertical pipe. Multiph. Sci. Technol. 36 (2), 55–73.
Liu, Q., Liu, S., Li, Y., Liu, Y., Wang, N., Yang, Q., Lu, H., 2024. Microbubble-based process for the enhancement of microfine and heavy oil droplets swirl separation in axial inlet hydrocyclone. Sep. Purif. Technol. 332, 125642.
Matsubayashi, T., Katono, K., Hayashi, K., Tomiyama, A., 2012. Effects of swirler shape on swirling annular flow in a gas-liquid separator. Nucl. Eng. Des. 249, 63–70.
Qiu, Z., Zhou, L., Bai, L., El-Emam, M.A., Agarwal, R., 2024. Empirical and numerical advancements in gas-liquid separation technology: a review. Geoenergy Sci. Eng. 233, 212577.
Syed, M.S., Rafeie, M., Henderson, R., Vandamme, D., Asadnia, M., Warkiani, M.E., 2017. A 3D-printed mini-hydrocyclone for high throughput particle separation. Lab a Chip 17 (14), 2459–2469.
Tsuchiya, K., Furumoto, A., Fan, L., Zhang, J., 1997. Suspension viscosity and bubble rise velocity in liquid-solid fluidized beds. Chem. Eng. Sci. 52 (18), 3053–3066.
Yajnik, K.S., Subbaiah, M.V., 1973. Experiments on swirling turbulent flows. Part 1. Similarity in swirling flows. J. Fluid Mech. 60, 665–687.
Yang, Q., Wang, H.L., Liu, Y., Li, Z.M., 2010. Solid/liquid separation performance of hydrocyclones with different cone combinations. Sep. Purif. Technol. 74, 271–279.
Yasuda, K., Haneda, K., 2015. Separation of oil droplets from oil-in-water emulsion using a microbubble generator. J. Chem. Eng. Jpn. 48 (3), 175–180.